

Supplement Information

Unexpected performance improvements of nitrogen dioxide and ozone sensors by including carbon monoxide sensor signal

Md Hasibul Hasan¹, Haofei Yu¹, Cesunica Ivey², Ajay Pillarisetti³, Ziyang Yuan⁴, Khanh Do⁵, Yi Li^{4*}

¹. Department of Civil, Environmental and Construction Engineering, University of Central Florida. Orlando, Florida, 32816, United States

². Department of Civil and Environmental Engineering, the University of California, Berkeley, Berkeley, California, 94720, United States

³. Environmental Health Sciences, School of Public Health, University of California, Berkeley, California, 94720, United States

⁴. Sailbri Cooper, Inc. Tigard, Oregon 97223, United States

⁵. Department of Chemical and Environmental Engineering, University of California, Riverside, California, 92521, United States

Table S1. Federal Reference Method/Federal Equivalent Method equipment lists at all six cities

City	Site ID	Pollutant	Model	Principle	Method Reference ID
Atlanta, GA	13-089-0002 ¹	CO	Thermo Scientific 48i-TLE	Infrared absorption	RFCA-0981-054
		NO ₂	Thermo Scientific 42i	Chemiluminescence	RFNA-1289-074
		O ₃	Thermo Scientific 49i	UV absorption	EQOA-0880-047
New York City, NY	36-081-0124 ²	CO	Teledyne API 300EU	Infrared absorption	RFCA-1093-093
		NO ₂	Thermo Scientific 42i	Chemiluminescence	RFNA-1289-074
		O ₃	Teledyne API T400	UV absorption	EQOA-0992-087
Phoenix, AZ	04-013-9997 ³	CO	Teledyne API 300EU	Infrared absorption	RFCA-1093-093
		NO ₂	Teledyne API T500U	Cavity Attenuated Phase Shift	EQNA-0514-212
		O ₃	Teledyne API T400	UV absorption	EQOA-0992-087
Portland, OR	41-051-0080 ⁴	CO	Teledyne API T300	Infrared absorption	RFCA-1093-093
		NO ₂	Teledyne API T500U	Cavity Attenuated Phase Shift	EQNA-0514-212
		O ₃	Teledyne API T400	UV absorption	EQOA-0992-087
RiverSide, CA	06-065-8005 ⁵	CO	Horiba APMA 360	Infrared absorption	RFCA-0895-106
		NO ₂	Thermo Scientific 42i	Chemiluminescence	RFNA-1289-074
		O ₃	Teledyne API 400E	UV absorption	EQOA-0992-087
Sacramento, CA	06-067-0010 ⁵	CO		N/A	
		NO ₂	Teledyne API 200 EU/501	Chemiluminescence	RFNA-1194-099
		O ₃	Teledyne API 400E	UV absorption	EQOA-0992-087

¹See Georgia Ambient Air Monitoring Plan for details: <https://airgeorgia.org/networkplans.html>

²See New York State Monitoring Network Plan for details: <https://www.dec.ny.gov/chemical/8406.html#Plan>

³See Maricopa County Air Monitoring Network Plan for details: <https://www.maricopa.gov/1669/Air-Monitoring-Network-Plans-and-Assessm>

⁴See Oregon Annual Ambient Criteria Pollutant Air Monitoring Network Plan for details:

<https://www.oregon.gov/deq/aq/Pages/Air-Quality-Monitoring.aspx>

⁵See California Annual Monitoring Network Report (<https://ww2.arb.ca.gov/our-work/programs/ambient-air-monitoring-regulatory/annual-monitoring-network-report>) and Quality Assurance Air Monitoring Site (<https://ww2.arb.ca.gov/applications/quality-assurance-air-monitoring-site-search-1>) for details

Table S2. Sensor performance (RMSE) at corresponding cities, without CO data

Pollutant		Portland	Atlanta	Riverside	Sacramento	New York	Phoenix
NO ₂	Linear	3.48	4.29	4.39	5.99	4.37	7.51
	Polynomial	2.78	4.19	4.56	5.09	3.74	6.66
	RF	2.72	3.16	3.75	3.91	3.43	5.46
O ₃	Linear	7.84	7.8	5.65	10.18	10.32	9.77
	Polynomial	7.66	8.29	6.6	10.68	10.62	10.44
	RF	5.70	6.68	5.14	6.85	9.28	8.31
CO	Linear	0.04	0.07	0.07		0.03	0.06
	Polynomial	0.04	0.07	0.07	N/A	0.03	0.05
	RF	0.03	0.04	0.03		0.02	0.05

RF = Random Forest

Table S3. Sensor performance (RMSE) at corresponding cities, with CO data introduced as an independent variable. Data shown in parentheses are changes of RMSE when CO data were included.

Pollutant		Portland	Atlanta	Riverside	Sacramento	New York	Phoenix
NO ₂	Linear	2.99(-0.49)	3.92(-0.37)	3.25(-1.14)	4.89(-1.1)	4.07(-0.3)	5.32(-2.19)
	Polynomial	2.69(-0.09)	3.93(-0.26)	3.66(-0.9)	4.92(-0.17)	4.21(0.47)	5.72(-0.94)
	RF	2.52(-0.2)	2.76(-0.4)	2.94(-0.81)	2.37(-1.54)	3.04(-0.39)	3.35(-2.11)
O ₃	Linear	6.02(-1.82)	7.34(-0.46)	5.54(-0.11)	7.02(-3.16)	6.4(-3.92)	6.98(-2.79)
	Polynomial	6.4(-1.26)	8.62(0.33)	6.96(0.36)	7.8(-2.88)	7.43(-3.19)	7.92(-2.52)
	RF	3.42(-2.28)	6.17(-0.51)	4.97(-0.17)	3.96(-2.89)	5.14(-4.14)	4.51(-3.8)

RF = Random Forest

Table S4. Parameters of all calibration models at six sites

		Linear	Polynomial	RF (Tree depth)
CO	PTL	$Cp=0.014Sp-0.002T-0.0001RH-5.19$	$Cp=2.65e-8Sp^3-1.38e-6T^3+1e-8RH^3-1.49$	6
	ATL	$Cp=0.009Sp-0.009T-0.002RH-3.07$	$Cp=1.86e-8Sp^3+6.22e-7T^3+8.12e-8RH^3-1$	6
	RAV	$Cp=0.006Sp+0.002T+0.0008RH-2.13$	$Cp=1.29e-8Sp^3+1.49e-6T^3+1.24e-7RH^3-0.71$	6
	SAC		N/A	
	NYC	$Cp=0.014Sp-0.002T-0.0004RH-5.41$	$Cp=2.96e-8Sp^3-1.54e-6T^3-1.8e-8RH^3-1.49$	4
	PHX	$Cp=0.014Sp-0.0006T-0.0008RH-5.41$	$Cp=2.69e-8Sp^3+1.04e-6T^3-2.79e-9RH^3-1.4$	4
NO ₂ (w/o CO)	PTL	$Cp=0.109Sp+0.05T-0.136RH-82.19$	$Cp=4.44e-8Sp^3+0.001T^3-3.53e-6RH^3-26.80$	5
	ATL	$Cp=0.009Sp-0.72T-0.154RH+31.73$	$Cp=7.56e-9Sp^3-0.0001T^3-3.38e-6RH^3+7.68$	6
	RAV	$Cp=-0.003Sp-0.986T-0.231RH+52.38$	$Cp=8.89e-10Sp^3-0.0001T^3-2.7e-6RH^3+12.71$	6
	SAC	$Cp=0.126Sp+0.464T-0.15RH-98.90$	$Cp=4.43e-8Sp^3+0.0004T^3-1.06e-5RH^3-19.96$	5
	NYC	$Cp=0.115Sp+0.33T-0.17RH-90.8$	$Cp=3.64e-8Sp^3+0.001T^3-8.56e-6RH^3-19.24$	6
	PHX	$Cp=0.036Sp-0.16T-0.135RH-5.12$	$Cp=1.77e-8Sp^3-9.44e-5T^3-1.09e-5RH^3+5.14$	4
NO ₂ (w CO)	PTL	$Cp=0.253CO+0.078Sp+0.011T-0.102RH-155.09$	$Cp=2.88e-7CO+3.71e-8Sp^3+0.0008T^3-3.17e-6RH^3-38.73$	5
	ATL	$Cp=-0.202CO+0.003Sp-0.644T-0.139RH-48.17$	$Cp=3.43e-7CO+4.75e-9Sp^3-0.0001T^3-3.55e-6RH^3-13.50$	6
	RAV	$Cp=0.4CO-0.023Sp-1.04T-0.179RH-91.60$	$Cp=7.26e-7CO-6e-9Sp^3-0.0001T^3+2.32e-6RH^3-29.65$	6
	SAC	$Cp=0.256CO+0.07Sp+0.18T-0.12RH+147.88$	$Cp=2.57e-7CO+3.33e-8Sp^3+0.0003T^3-8.9e-6RH^3-28.10$	5
	NYC	$Cp=0.364CO+0.088Sp+0.127T-0.141RH-205.43$	$Cp=2.68e-7CO+3.33e-8Sp^3+0.0008T^3-8.18e-6RH^3-31.97$	6
	PHX	$Cp=0.307CO+0.019Sp-0.007T-0.133RH-118.37$	$Cp=4.6e-7CO+1.1e-8Sp^3-8.82e-5T^3-0.128RH^3-16.52$	4
O ₃ (w/o CO)	PTL	$Cp=0.121Sp+0.545T-0.289RH-92.78$	$Cp=3.42e-8Sp^3+0.0027T^3-9.93e-6RH^3-22.63$	6
	ATL	$Cp=0.026Sp+0.669T-0.662RH+21.28$	$Cp=5.57e-9Sp^3+0.0006T^3-2.88e-5RH^3+12.69$	4
	RAV	$Cp=0.021Sp+4.71T+0.39RH-134.42$	$Cp=3.76e-9Sp^3+0.0011T^3-2.66e-5RH^3+10.09$	4
	SAC	$Cp=0.014Sp+1.45T-0.186RH-11.03$	$Cp=1.26e-9Sp^3+0.0013T^3-1.08e-5RH^3+11.31$	5
	NYC	$Cp=0.022Sp+0.72T-0.23RH+10.9$	$Cp=5.3e-9Sp^3+0.002T^3-1.36e-5RH^3+21.86$	4
	PHX	$Cp=-9.8e-4Sp+1.16T-0.205RH+14.25$	$Cp=-8.85e-10Sp^3+0.001T^3-1.35e-5RH^3+16.34$	6

O ₃ (w CO)	PTL	$Cp=-0.56CO+0.088Sp+0.32T-0.27RH+167.89$	$Cp=-1.01e-6CO+2.64e-8Sp3+0.0021T3-9.44e-6RH3+53.18$	6
	ATL	$Cp=-0.3CO+0.034Sp+0.64T-0.62RH+130.34$	$Cp=-5.87e-7CO+6.86e-9Sp3+0.0005T3-3e-5RH3+50.85$	4
	RAV	$Cp=-0.138CO+0.024Sp+4.47T+0.34RH-74.42$	$Cp=-6.31e-7CO+4.94e-9Sp3+0.001T3-2.78e-5RH3+51.25$	4
	SAC	$Cp=-0.35CO+0.038Sp+1.12T-0.152RH+109.38$	$Cp=-6.52e-7CO+9.21e-9Sp3+0.001T3-1.22e-5RH3+46.43$	5
	NYC	$Cp=-1.11CO+0.029Sp+0.923T-0.129RH+427.19$	$Cp=-2.17e-6CO+6.9e-9Sp3+0.0023T3-8.06e-6RH3+144.1$	4
	PHX	$Cp=-0.35CO+0.003Sp+0.661T-0.171RH+161.36$	$Cp=-6.67e-7CO+9.5e-10Sp3+0.0008T3-1.17e-5RH3+62.15$	6

Table S5. Results of NO₂ and O₃ LCAQ sensors tested by AQ-SPEC (only electrochemical type sensors are included, data retrieved on March 5th, 2022)

Make (Model)	Pollutant	Field R ²
APIS	NO ₂	0.30 to 0.44
	O ₃	0.73 to 0.83
AQMesh (v4.0)	NO ₂	0.0 to 0.46
	O ₃	0.46 to 0.83
AQMesh (v5.1)	NO ₂	0.49 to 0.54
	O ₃	0.62 to 0.74
Igienair (Zaack AQI)	NO ₂	0.53 to 0.58
	O ₃	0.0
Kunak	NO ₂	0.24 to 0.32
	O ₃	0.86 to 0.88
Magnasci SRL	NO ₂	0.00 to 0.05
	O ₃	0.00 to 0.08
Oizom (Polludrone Smart)	NO ₂	0.002 to 0.03
	O ₃	0.14 to 0.23
Perkin Elmer (ELM)	NO ₂	0.0
	O ₃	0.89 to 0.96
Spec Sensors	NO ₂	0.0 to 0.16
	O ₃	0.0 to 0.24
Vaisala (AQT410) Ver. 1.11	NO ₂	0.0
	O ₃	0.40 to 0.58
Vaisala (AQT410) Ver. 1.15	NO ₂	0.43 to 0.61
	O ₃	0.66 to 0.82

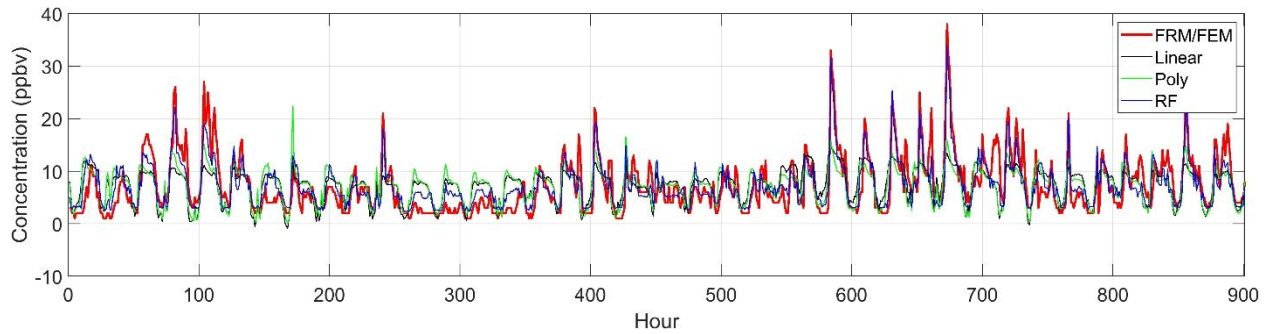


Figure S1. Time-series plot of hourly NO_2 concentrations at Atlanta as collected by FRM/FEM equipment, and from low-cost sensors with linear, polynomial, and random forest calibration

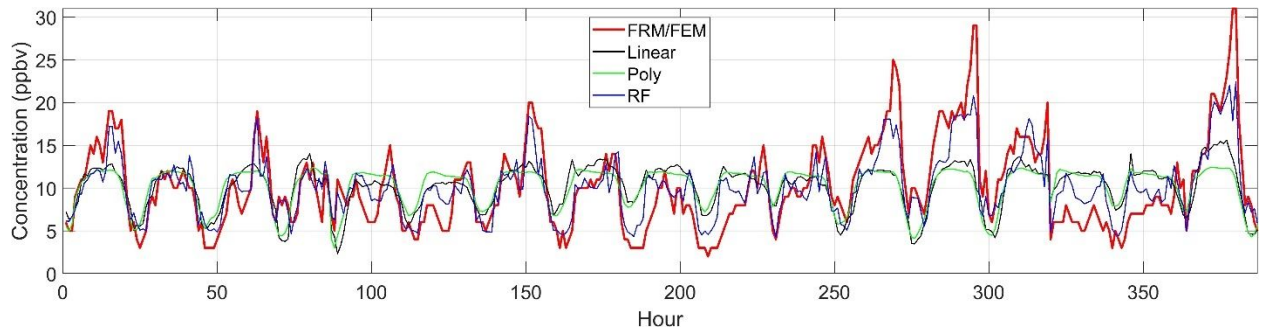


Figure S2. Time-series plot of hourly NO_2 concentrations at Riverside as collected by FRM/FEM equipment, and from low-cost sensors with linear, polynomial, and random forest calibration

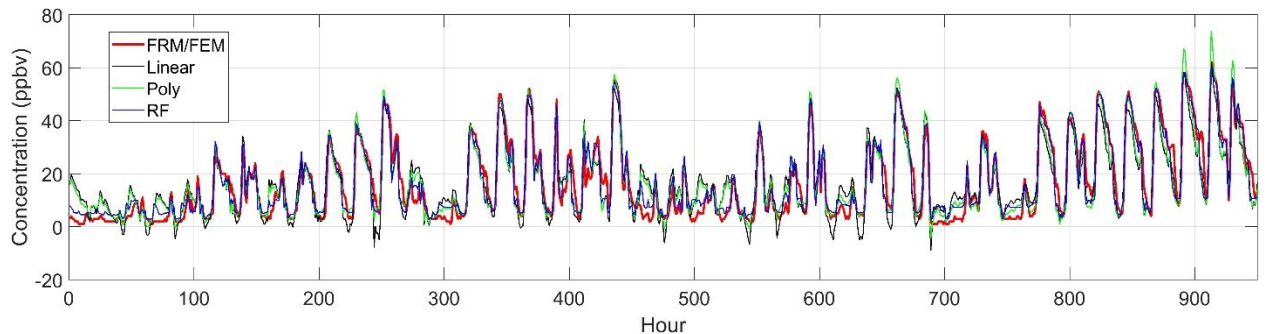


Figure S3. Time-series plot of hourly NO_2 concentrations at Sacramento as collected by FRM/FEM equipment, and from low-cost sensors with linear, polynomial, and random forest calibration

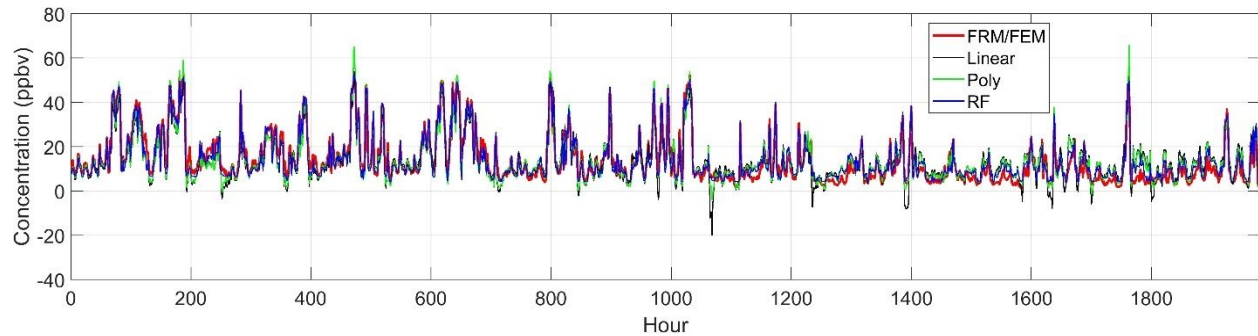


Figure S4. Time-series plot of hourly NO₂ concentrations at New York City as collected by FRM/FEM equipment, and from low-cost sensors with linear, polynomial, and random forest calibration

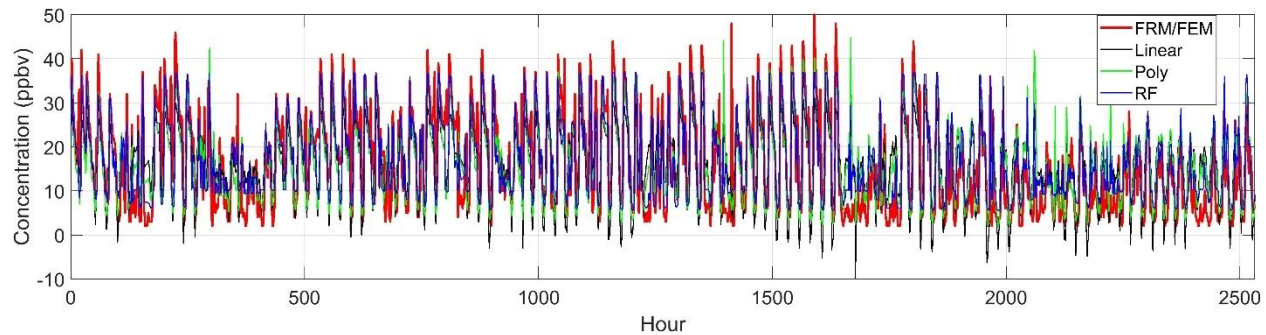


Figure S5. Time-series plot of hourly NO₂ concentrations at Phoenix as collected by FRM/FEM equipment, and from low-cost sensors with linear, polynomial, and random forest calibration

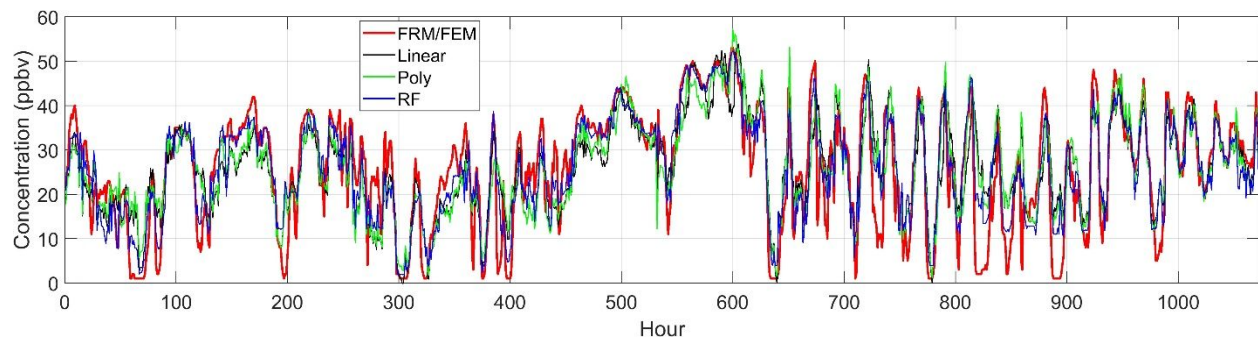


Figure S6. Time-series plot of hourly O₃ concentrations at Portland as collected by FRM/FEM equipment, and from low-cost sensors with linear, polynomial, and random forest calibration

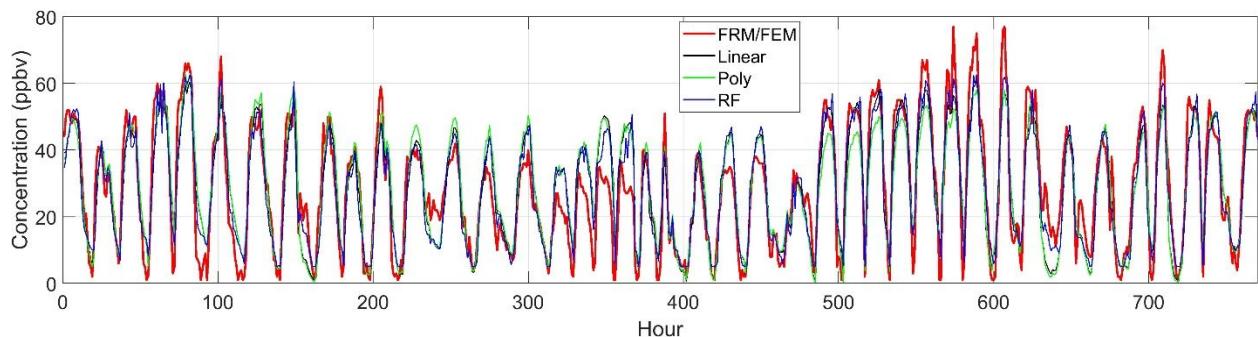


Figure S7. Time-series plot of hourly O₃ concentrations at Atlanta as collected by FRM/FEM equipment, and from low-cost sensors with linear, polynomial, and random forest calibration

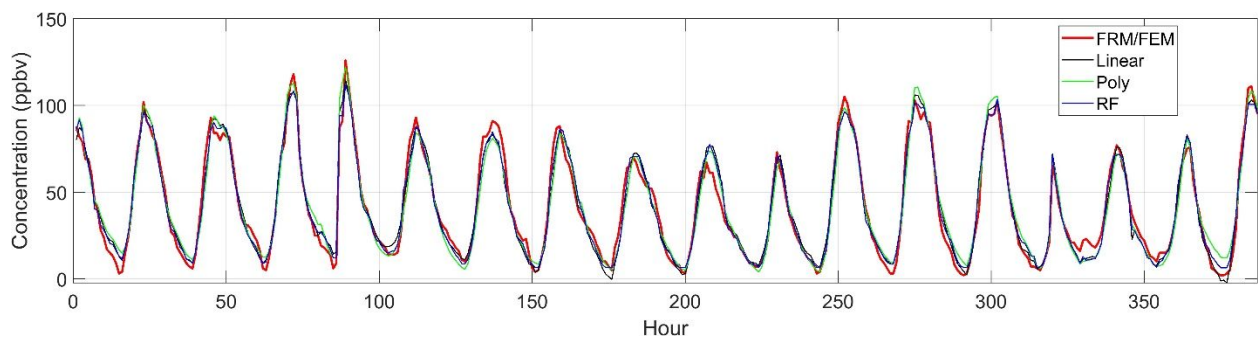


Figure S8. Time-series plot of hourly O₃ concentrations at Riverside as collected by FRM/FEM equipment, and from low-cost sensors with linear, polynomial, and random forest calibration

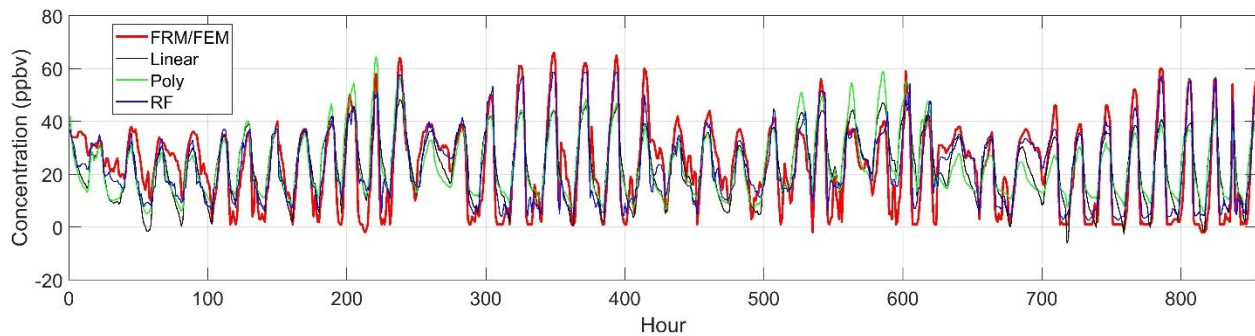


Figure S9. Time-series plot of hourly O_3 concentrations at Sacramento as collected by FRM/FEM equipment, and from low-cost sensors with linear, polynomial, and random forest calibration

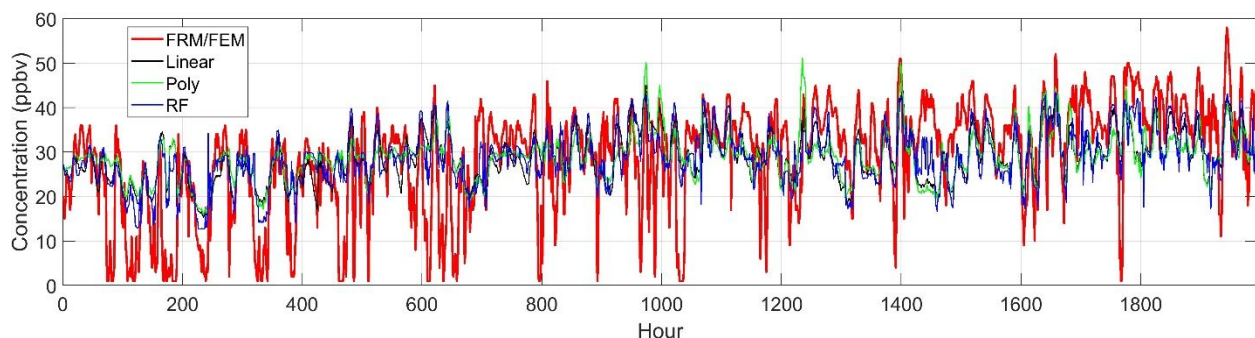


Figure S10. Time-series plot of hourly O_3 concentrations at New York City as collected by FRM/FEM equipment, and from low-cost sensors with linear, polynomial, and random forest calibration

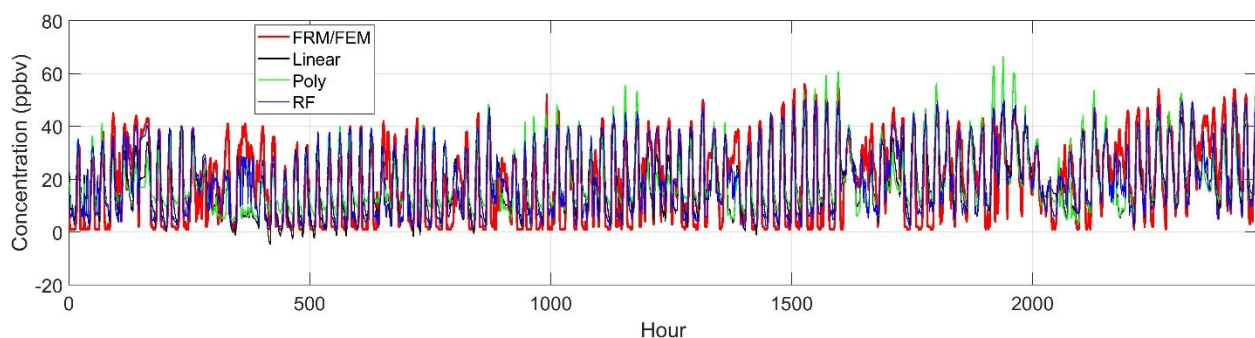


Figure S11. Time-series plot of hourly O_3 concentrations at Phoenix as collected by FRM/FEM equipment, and from low-cost sensors with linear, polynomial, and random forest calibration